Estimating Various Response Spectra from a Fourier Amplitude Spectrum

Rui Zhang[1], Haizhong Zhang*[2], and Yan-Gang Zhao[3]

ABSTRACT

Response spectra, including spectral displacement (SD), spectral velocity (SV), and spectral acceleration (SA) are important ground-motion intensity measures. To estimate ground motions in regions lacking earthquake data, a modeling approach based on random vibration theory (RVT) that combines a model of the Fourier amplitude spectrum (FAS) and a ground-motion duration model is an attractive tool. However, this RVT-based approach is currently limited to estimating SD or pseudospectral acceleration. This study aimed to develop a new approach capable of estimating various response spectra from the FAS, including not only SD but also SV and SA, based on the RVT framework. First, equations for estimating SV and SA from the FAS were derived by replacing the oscillator transfer function for SD in the traditional RVT framework with those for SV and SA, respectively. Moreover, two simple modification factors for the duration of the root mean square oscillator response were introduced to ensure that the SV and SA from the RVT approach matched those from the time-series analysis. The proposed approach maintains the use of the RVT framework for estimating SD without introducing any additional concepts; however, it can readily provide three types of response spectra simultaneously.

KEY POINTS

- We develop a new method for estimating different response spectra from the Fourier amplitude spectrum (FAS).
- Our proposed approach for calculating spectral velocity (SV) and spectral acceleration (SA) has high accuracy.
- Our new method can be used in seismic hazard studies, especially in region with limited earthquake data.

INTRODUCTION

Response spectra, including spectral displacement (SD), spectral velocity (SV), and spectral acceleration (SA), are important ground-motion intensity measures. For example, SA and pseudospectral acceleration (PSA) converted from SD have been widely used in seismic designs (Eurocode 8, 2004; Fujiwara *et al.*, 2006; ASCE/SEI7-10, 2011; GB 18306-2015, 2015; GB 50011-2010, 2016; Zhang and Zhao, 2022). In addition, in the seismic design of structures incorporating supplemental velocity-dependent dampers, SV plays a critical role in determining the peak relative velocity values across the ends of the dampers (Federal Emergency Dissipation Agency [FEMA-450], 2003; Desai and Tande, 2017; Liu *et al.*, 2025). Furthermore, SV is also essential for conducting seismic analysis of structures exhibiting nonproportional damping, particularly within the framework of the complex mode response spectrum method (Zhou *et al.*, 2004; Yu and Zhou, 2008).

Generally, to determine the response spectra for seismic design, ground-motion prediction equations (GMPEs) are required to implement probability seismic hazard analyses. In principle, the GMPE for a specific region can be derived by regression analysis of the numerous earthquake data recorded in this region. However, many regions worldwide have insufficient earthquake data for generating a region-specific empirical GMPE. In addition, using GMPEs from other regions with rich earthquake data can often lead to unrealistic estimates of ground-motion response spectra because of the different seismological characteristics of the different regions (Bora *et al.*, 2014, 2016).

Hanks and McGuire (1981) proposed a modeling approach for estimating PGA based on random vibration theory (RVT) by combining a model of the Fourier amplitude spectrum (FAS) and a ground-motion duration model, which is particularly suitable for regions lacking earthquake data. Furthermore, Boore (1983, 2003) extended this approach to estimate the PGV and PSA or SD. Many studies (Boore and Atkinson, 1987; Toro and McGuire, 1987; Campbell, 2003) utilized the

1. School of Geography and Tourism, Qilu Normal University, Jinan, China; 2. Yamagata University, Yamagata, Japan; 3. Faculty of Architecture, Civil and Transportation Engineering, Beijing University of Technology, Beijing, China

*Corresponding author: zhang@tds1.tr.yamagata-u.ac.jp

Cite this article as Zhang, R., H. Zhang, and Y.-G. Zhao (2025). Estimating Various Response Spectra from a Fourier Amplitude Spectrum, *Bull. Seismol. Soc. Am.* **XX**, 1–15, doi: 10.1785/0120240242

RVT-based approach to develop GMPEs for PGA and SD in Eastern North America, where strong-motion recordings are limited. Moreover, the RVT-based approach was used to construct GMPEs for PSA, PGA, and PGV in the Next Generation Attenuation for Central and Eastern North America (CENA) project (NGA-EAST) (PEER Report, 2015). Similarly, Lavrentiadis and Abrahamson (2023) applied the RVT-based approach to develop nonergodic GMPEs for PSA. Kottke *et al.* (2021) provided recommendations regarding the application of the RVT-based approach in the development of GMPEs. In addition to its application in the development of GMPEs, the RVT-based approach has found widespread application in many other areas. Bora *et al.* (2016) used RVT to explore the relationship between the Fourier and response spectra of ground motion. Rathje and Ozbey (2006) extended the RVT approach to a site response analysis. Zhang and Zhao (2020, 2021a,b,c) also utilized the RVT approach to discuss the relationships between different types of spectra as well as the damping modification factor of the response spectra. Furthermore, Zhao *et al.* (2023) and Zhang *et al.* (2023) introduced the RVT approach to a probabilistic seismic hazard analysis framework. However, currently, the RVT-based approach is limited to the estimation of SD or PSA and is unavailable for estimating SV and SA. Although Zhang and Zhao (2021a,b) used the RVT approach to estimate SA and SV from the FAS by simply replacing the oscillator transfer function, its accuracy has never been discussed.

This study aims to develop a new approach capable of estimating various response spectra, including not only SD but also SV and SA, from the FAS based on the RVT framework. The remainder of this article is organized as follows. First, the theoretical framework for estimating SD using the FAS based on RVT is briefly reviewed. Then, an approach to estimate various response spectra from the FAS is presented. Subsequently, the results of the proposed approach are compared with those of a time-series analysis considering a wide range of oscillator periods, magnitudes, and distances. Finally, the conclusions of this study are summarized.

APPROACH FOR ESTIMATING SD OR PSA FROM THE FAS BASED ON RVT

Boore (2003) applied RVT to estimate SD or PSA from the FAS. The RVT approach states that the peak value ($y_{\max}$) of a time-series signal is equal to its root mean square (rms) value y_{rms}, multiplied by a peak factor p_f, that is, $y_{\max} = p_f \times y_{\mathrm{rms}}$. Because SD represents the peak value of the oscillator-response displacement, it equals the rms value of the oscillator-response displacement multiplied by a corresponding peak factor:

$$\mathrm{SD}(\omega) = p_f \sqrt{\frac{1}{\pi D_{\mathrm{rms}}} \int_0^{\infty} |Y_{\mathrm{SD}}(\omega)|^2 \mathrm{d}\omega}, \qquad (1)$$

in which ω is the circular frequency of the ground motion, and the square root part represents the rms value of the oscillator-response displacement, which is obtained from the FAS of this displacement $Y_{\mathrm{SD}}(\omega)$, according to Parseval's theorem. In addition, $Y_{\mathrm{SD}}(\omega)$ can be obtained from the FAS of ground-motion acceleration $Y(\omega)$ via

$$Y_{\mathrm{SD}}(\omega) = Y(\omega)|H_{\mathrm{SD}}(\omega,\bar{\omega},\xi)|, \qquad (2)$$

in which $H_{\mathrm{SD}}(\omega,\omega,\xi)$ is the oscillator transfer function for the displacement response,

$$|H_{\mathrm{SD}}(\omega,\bar{\omega},\xi)| = \frac{1}{\sqrt{(2\xi\omega\bar{\omega})^2 + (\omega^2 - \bar{\omega}^2)^2}}, \qquad (3)$$

in which ω and ξ are the circular frequency and damping ratio for a single-degree-of-freedom oscillator, respectively.

In equation (1), p_f is the peak factor model defined as the ratio of the peak oscillator response to the rms oscillator response. Several peak factor models have been developed for RVT analysis (Cartwright and Longuet-Higgins, 1956; Davenport, 1964; Vanmarcke, 1975; Wang and Rathje, 2016). Although the Cartwright and Longuet-Higgins (1956) model has been commonly applied in engineering seismology and site-response analyses, the Vanmarcke (Vanmarcke, 1975) model provides better estimates of the peak factor (Wang and Rathje, 2016). The cumulative distribution function of the peak factor p_f provided by Vanmarcke (Vanmarcke, 1975) is expressed as follows:

$$P(p_f < r) = \left[1 - \exp(-r^2/2)\right] \exp\left\{-2f_z \exp(-r^2/2) D_{\mathrm{gm}} \frac{[1 - \exp(-\sqrt{\pi/2}\delta^{1.2} r)]}{1 - \exp(-r^2/2)}\right\}, \qquad (4)$$

in which D_{gm} is the duration of the ground motion, which is related to the corner frequency f_c and distance R and is expressed as $D_{gm} = 1/f_c + 0.05R$ (Herrmann, 1985; Atkinson and Silva, 2000). δ is the bandwidth factor of the FAS, which is defined as a function of the spectral moments of the FAS:

$$\delta = \sqrt{1 - \frac{(m_1)^2}{m_0 \times m_2}}, \qquad (5)$$

in which m_n ($n = 0, 1, 2$) denotes the nth order spectral moment of the square of the FAS, defined by

$$m_n = \frac{1}{\pi} \int_0^{\infty} \omega^n |Y_{\mathrm{SD}}(\omega)|^2 \mathrm{d}\omega. \qquad (6)$$

In equation (4), f_z is the rate of zero crossing, defined as follows:

$$f_z = \frac{1}{2\pi} \sqrt{\frac{m_2}{m_0}}. \qquad (7)$$

In the RVT analysis, the expected value of p_f is typically used. According to equation (4), the expected value p_f is obtained as follows:

$$\overline{p_f} = \int_0^\infty 1 - P(p_f < r)\mathrm{d}r. \qquad (8)$$

In equation (1), D_{rms} represents the rms duration for SD or PSA, which is used to modify the basic assumptions underlying RVT. Boore and Joyner (1984) proposed an equation for estimating D_{rms} from D_{gm} by comparing the pseudovelocity response spectra computed from time-series analysis and RVT. Liu and Pezeshk (1999) improved the D_{rms} model by considering various magnitudes, distances, and damping ratios. Boore and Thompson (2012) derived another equation for D_{rms} for a large range of magnitudes, distances, periods, and seismological models by comparing the PSA computed from time-series analysis and RVT. Subsequently, Boore and Thompson (2015) further modified the coefficients of the D_{rms} model by Boore and Thompson (2012), and D_{rms} is expressed as

$$D_{\mathrm{rms}} = D_{\mathrm{gm}}\left(c_1 + c_2\frac{1-\eta^{c_3}}{1+\eta^{c_3}}\right)\left[1 + \frac{c_4}{2\pi\xi}\left(\frac{\eta}{1+c_5\eta^{c_6}}\right)^{c_7}\right], \qquad (9)$$

in which c_i, $i = 1, 2, 3, \ldots, 7$ are coefficients (Boore and Thompson, 2012, 2015), $\eta = T/D_{\mathrm{gm}}$, and T is the oscillator period.

As shown in equation (1), this RVT-based approach was developed for the estimation of SD or PSA (PSA $= \omega^2$SD) and requires some modifications to estimate SV and SA.

PROPOSED APPROACH FOR ESTIMATING SA AND SV FROM THE FAS BASED ON RVT

Estimating SA and SV based on RVT

As described earlier, SD is calculated as the product of the rms value of the oscillator-response displacement with a corresponding peak factor. Similarly, SA was thought to be equal to the rms value of the oscillator-response acceleration multiplied by the corresponding peak factor. Furthermore, SV could also be determined using a similar approach, in which it equals the rms value of the oscillator-response velocity multiplied by the corresponding peak factor:

$$\mathrm{SV} = p_f\sqrt{\frac{1}{\pi D_{\mathrm{SV}}}\int_0^\infty |Y_{\mathrm{SV}}(\omega)|^2\mathrm{d}\omega}, \qquad (10)$$

$$\mathrm{SA} = p_f\sqrt{\frac{1}{\pi D_{\mathrm{SA}}}\int_0^\infty |Y_{\mathrm{SA}}(\omega)|^2\mathrm{d}\omega}. \qquad (11)$$

In equation (10), $Y_{\mathrm{SV}}(\omega)$ is the FAS of the oscillator-response velocity, which can be obtained using $Y_{\mathrm{SV}}(\omega) = Y(\omega) \times |H_{\mathrm{SV}}(\omega)|$, and $|H_{\mathrm{SV}}(\omega)|$ is the absolute value of the oscillator transfer function for the oscillator-response velocity (Zhang and Zhao, 2021b), expressed as follows:

$$|H_{\mathrm{SV}}(\omega)| = \frac{\omega}{\sqrt{(2\xi\omega\bar{\omega})^2 + (\omega^2 - (\bar{\omega})^2)^2}}. \qquad (12)$$

In equation (11), $Y_{\mathrm{SA}}(\omega)$ is the FAS of the oscillator-response acceleration, which can be obtained using $Y_{\mathrm{SA}}(\omega) = Y(\omega)|H_{\mathrm{SA}}(\omega)|$, and $|H_{\mathrm{SA}}(\omega)|$ is the absolute value of the oscillator transfer function for the absolute oscillator-response acceleration (Zhang and Zhao, 2021a), expressed as follows:

$$|H_{\mathrm{SA}}(\omega)| = \frac{\sqrt{(2\xi\omega\bar{\omega})^2 + (\bar{\omega})^4}}{\sqrt{(2\xi\omega\bar{\omega})^2 + (\omega^2 - (\bar{\omega})^2)^2}}. \qquad (13)$$

In equations (10) and (11), p_f denotes the peak factor, which can be calculated using equations (4)–(8). When computing the peak factor p_f for SA, the nth order spectral moments m_n should be calculated using $Y_{\mathrm{SA}}(\omega)$ instead of $Y_{\mathrm{SD}}(\omega)$ in equation (6). Similarly, when computing the peak factor p_f for SV, the nth order spectral moments m_n should be calculated using $Y_{\mathrm{SV}}(\omega)$ instead of $Y_{\mathrm{SD}}(\omega)$ in equation (6).

Similar to the estimation of SD or PSA using RVT, some basic assumptions are made when applying RVT to estimate SA and SV, such as the quasi stationarity of the equivalent time series and the statistical independence of consecutive maxima of the time series (Boore and Joyner, 1984; Liu and Pezeshk, 1999; Boore and Thompson, 2012). These assumptions are not inherently satisfied by seismic ground motions, leading to discrepancies between RVT and time-series analysis. To overcome these limitations, D_{rms} was proposed to correct errors in SD arising from these assumptions (Boore and Joyner, 1984; Liu and Pezeshk, 1999; Boore and Thompson, 2012, 2015). However, D_{rms} was derived by matching the SD from the RVT with that from time-series analysis without ensuring consistency for SV and SA. To resolve this issue, D_{SV} and D_{SA}, denoting the rms duration for SV and SA, respectively, are introduced in equations (10) and (11) to address errors in SA and SV caused by the assumptions underlying RVT.

The rms duration models for SV and SA

To derive the D_{SV} and D_{SA} models, SV and SA were analyzed using time-series analysis and RVT modeling. The FAS model of Boore (2003) was used as the ground-motion input for the RVT modeling. The parameter values required for the FAS model in the Eastern North America region were selected according to Boore and Thompson (2015) and Wang and Rathje (2016) and are listed in Table 1. The adopted crust amplification $A(f)$, geometrical spreading $Z(R)$, and path attenuation in the FAS model are listed in Table 1 (Zhang and Zhao, 2020). For the time-series analysis, 10,000 time series were generated for each corresponding FAS using the SMSIM (Boore, 2005) program. The generated time series

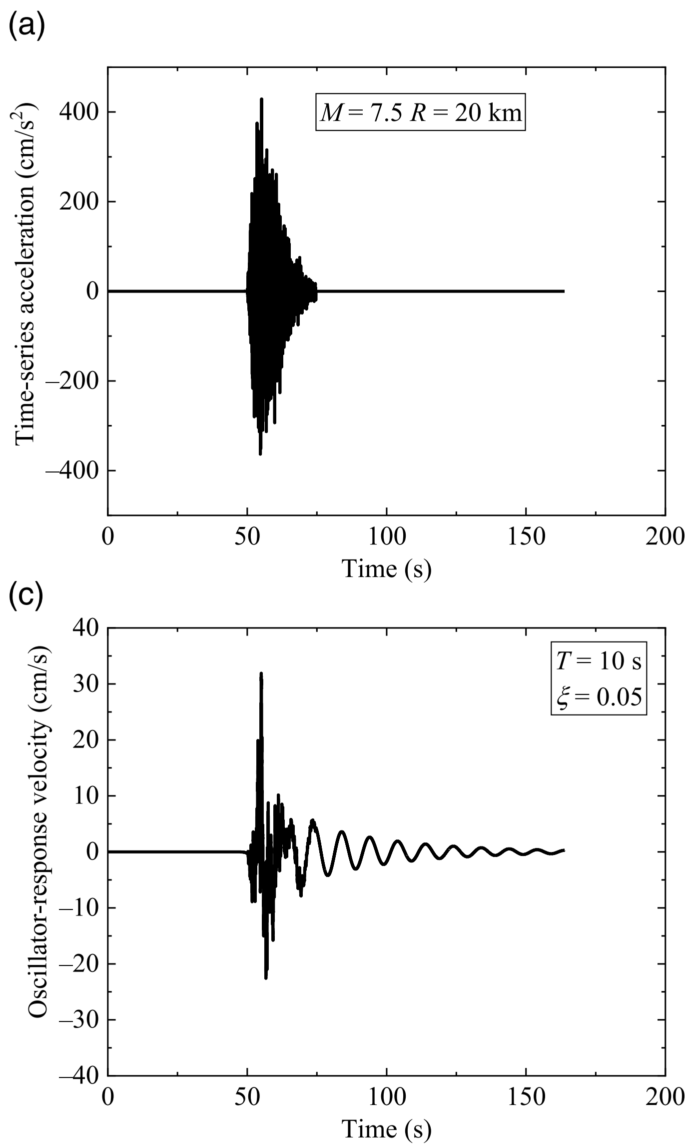

Figure 1. (a) A generated time series for *M* 7.5 and *R* = 20 km, (b) oscillator-response acceleration, (c) oscillator-response velocity, and (d) oscillator-response displacement for an oscillator period of 10 s.

includes a long tail to ensure that the oscillator response approaches zero at the end, allowing for the capture of the peak response, as shown in Figure 1. A large range of magnitudes from 4 to 8, with an interval of 0.5, source-to-site distances ranging from 20 to 200.01 km, and oscillator periods from 0.1 to 10 s with an interval of 0.01 s were considered. In addition, a damping ratio of 5% is used for the analyses because similar to Boore (2003), this study focuses on response spectra with a 5% damping ratio. The reason for excluding other damping ratios is primarily because spectral values are commonly defined for a 5% damping ratio in both seismic design and structural dynamics analysis. If SA, SV, and SD with damping ratios other than 5% are required, the values for a 5% damping ratio can be adjusted using the corresponding damping modification factors for SA, SV, and SD, respectively (Conde-Conde and Benavent-Climent, 2019).

In principle, D_{SV} and D_{SA} should also be derived by matching the SV and SA from the RVT modeling with those from the time-series analysis. Because D_{SV} and D_{SA}, similar to D_{rms}, are

TABLE 1
Parameters Used in the Fourier Amplitude Spectral Model

Parameters	Value
Density of crust ρ(g/cm^3)	2.8
Stress drop $\Delta\sigma$(bar)	400
Shear-wave velocity of crust β(km/s)	3.7
Site diminution k_0 (s)	0.006
Crust amplification $A(f)$	Boore and Thompson (2015)
Geometrical spreading $Z(R)$	Atkinson and Boore (2014)
Path attenuation	Atkinson and Boore (2014)

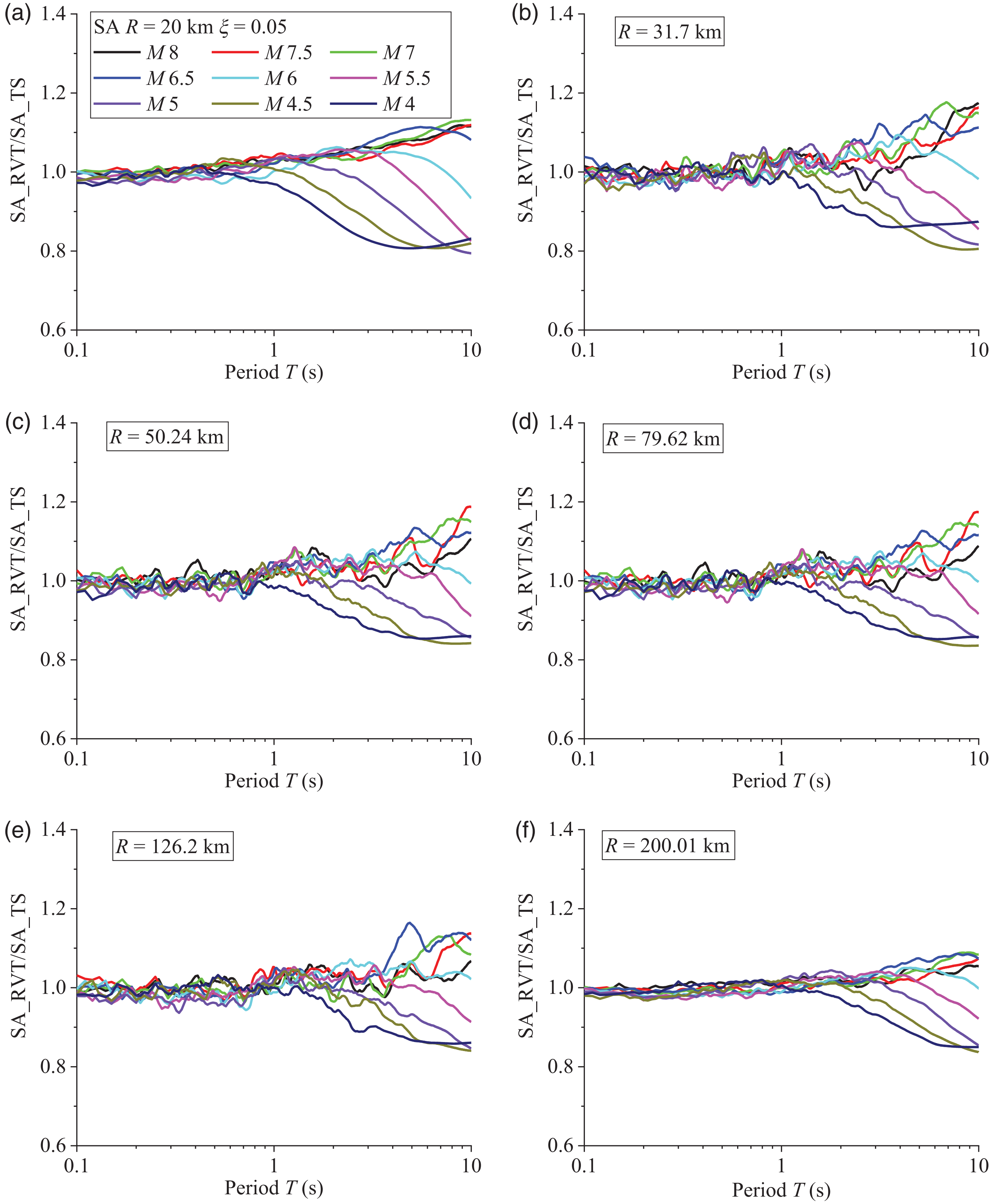

Figure 2. Ratio between spectral acceleration (SA) computed using random vibration theory (RVT) modeling (assuming $D_{SA} = D_{rms}$) and time-series analysis considering various magnitudes, distances, and periods.

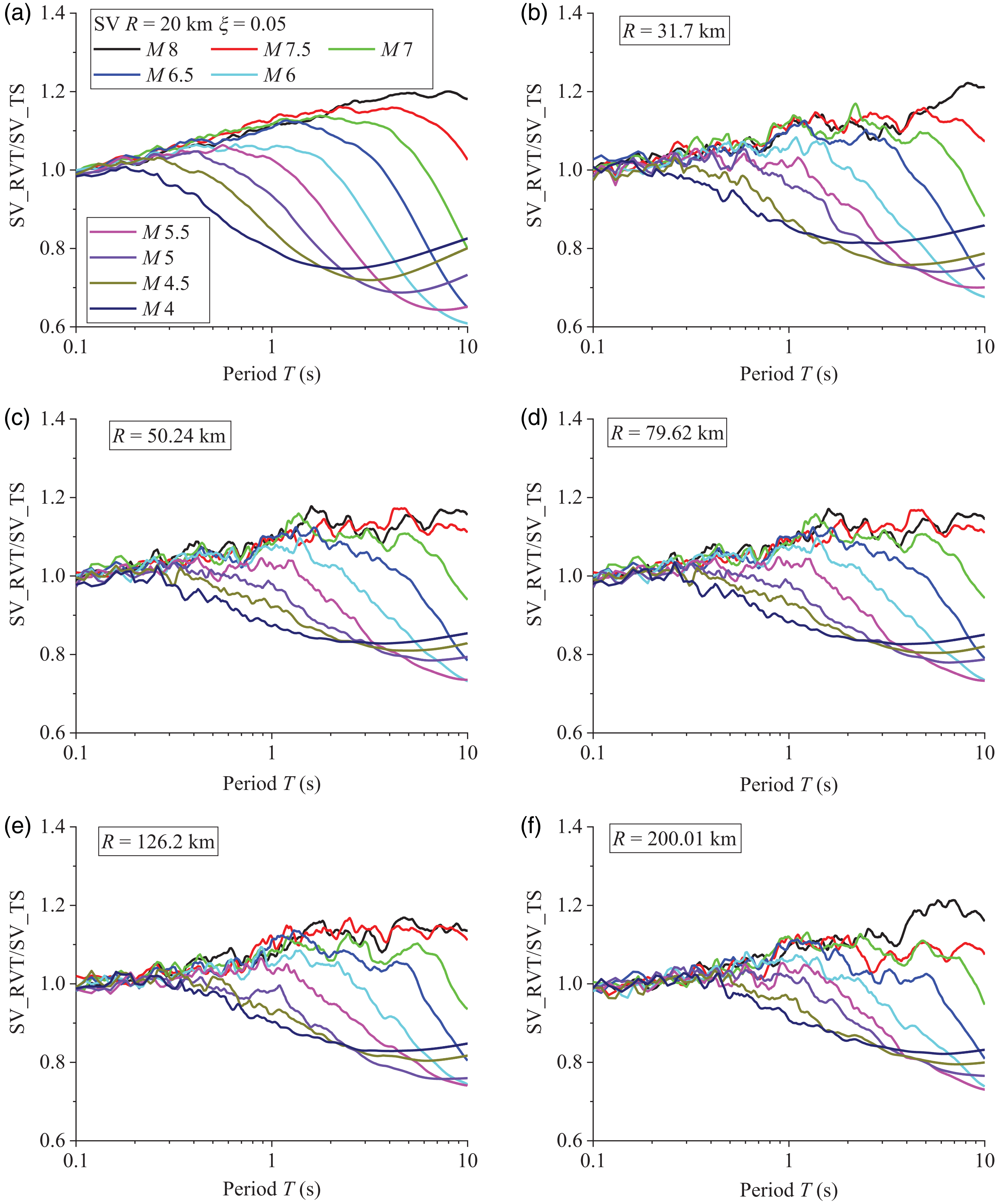

Figure 3. Ratio between spectral velocity (SV) computed using RVT modeling (assuming $D_{SV} = D_{rms}$) and time-series analysis considering various magnitudes, distances, and periods.

TABLE 2
Values of the Parameters k_1, k_2, and k_3 in Equation (17)

	R (km)					
13 **M**	**20**	**31.7**	**50.24**	**79.62**	**126.2**	**200.01**
4	−0.2, 0.24, 0.8	0.18, 0.18, 0.86	−0.17, 0.15, 0.88	−0.19, 0.16, 0.89	−0.22, 0.17, 0.9	−0.22, 0.14, 0.91
4.5	−0.43, 0.4, 0.84	−0.35, 0.27, 0.87	−0.27, 0.18, 0.91	−0.28, 0.18, 0.92	−0.29, 0.18, 0.93	−0.28, 0.14, 0.94
5	−0.59, 0.41, 0.9	−0.48, 0.28, 0.95	−0.33, 0.17, 0.95	−0.34, 0.16, 0.95	−0.33, 0.13, 0.95	−0.33, 0.08, 0.99
5.5	−0.59, 0.22, 1	−0.39, 0.07, 0.99	−0.31, 0.02, 1.01	−0.3, 0, 1.01	−0.26, −0.04, 1.02	−0.25, −0.06, 1.02
6	−0.3, −0.21, 1.06	−0.21, −0.21, 1.06	−0.13, −0.23, 1.06	−0.11, −0.24, 1.06	−0.06, −0.3, 1.07	−0.12, −0.2, 1.07
6.5	0.1, −0.6, 1.12	0.18, −0.57, 1.1	0.16, −0.47, 1.09	0.17, −0.47, 1.09	0.2, −0.48, 1.09	0.09, −0.34, 1.08
7	0.26, −0.57, 1.13	0.22, −0.41, 1.11	0.2, −0.33, 1.09	0.2, −0.32, 1.09	0.19, −0.29, 1.08	0.14, −0.23, 1.09
7.5	0.2, −0.27, 1.13	0.14, −0.15, 1.1	0.16, −0.13, 1.09	0.16, −0.13, 1.08	0.15, −0.12, 1.1	0.01, 0, 1.08
8	0.18, −0.1, 1.11	−0.01, 0.15, 1.09	0.04, 0.02, 1.1	0.04, 0.02, 1.09	0.11, −0.06, 1.09	0.15, −0.03, 1.08

also introduced to modify the basic assumptions underlying RVT, they are expected to be similar in terms of basic function form and controlling factors. Because of the success of Boore and Thompson (2015) in developing the D_{rms}, D_{SV}, and D_{SA} are preferred to be developed based on D_{rms} (equation 9). First, to investigate the accuracy of ignoring the difference between the rms durations for SV and SA with that for SD, SV, and SA were calculated based on the RVT modeling, assuming that D_{SV} and D_{SA} were equal to D_{rms}. The ratios of SA and SV calculated using the time-series analysis and RVT modeling are shown in Figures 2 and 3, respectively. As shown in Figure 2, when the oscillator period T was smaller than 1 s, the results obtained using D_{rms} instead of D_{SA} based on RVT closely matched those from the time-series analysis. This suggests that assuming D_{rms} equals D_{SA} is appropriate for the period $T < 1$ s. However, for $T > 1$ s, the error between the results of the RVT modeling and the time-series analysis increased with an increase in the oscillator period. At an oscillator period of $T = 10$ s, the maximum error between the results of the RVT simulation and time-series analysis reached 19.4%. This indicates that using D_{rms} to replace D_{SA} can result in significant errors when the oscillator period $T > 1$ s. Furthermore, when the oscillator period $T > 1$ s, the error between the results of the RVT modeling and the time-series analysis was also dependent on the magnitude and distance. For smaller magnitudes, the results of RVT were smaller than those of the time-series analysis, whereas for larger magnitudes, the results of RVT were larger than those of the time-series analysis. With increasing source-to-site distance, the error between the results of RVT and the time-series analysis decreased slightly.

As shown in Figure 3, ignoring the difference between the rms durations for SV and SD can lead to significant errors. The error between the SV computed by RVT and the time-series analysis increased with the oscillator period. This error reached 34.6% at an oscillator period of $T = 10$ s. This indicates that using D_{rms} to replace D_{SV} led to significant discrepancies, particularly over long periods. Furthermore, the figure illustrates that these errors were also dependent on the magnitude and source-to-site distance. As the source-to-site distance increased, the errors decreased slightly. In addition, for smaller magnitudes, the results of RVT were smaller than those of the time-series analysis, whereas for larger magnitudes, the results of RVT were larger than those of the time-series analysis.

In addition, SD was also calculated using both time-series analysis and RVT, adopting the rms duration D_{rms}. The SD estimation using D_{rms} demonstrates high accuracy, with an average error not exceeding 3%, consistent with the conclusions of Boore and Thompson (2015). Because the accuracy of SD estimation using RVT has been extensively discussed by Boore and Thompson (2015), the SD-related results are not presented in this article.

From the aforementioned analyses, it can be concluded that although the direct use of D_{rms} to replace D_{SV} and D_{SA} was inappropriate, the errors were not considerably large and were limited to 19.4% and 34.6%, respectively. Therefore, this study constructed D_{SV} and D_{SA} models based on the D_{rms} model by simply introducing two adjusting factors: MF_{SA} and MF_{SV}. 2

$$D_{SV} = MF_{SV} \cdot D_{rms}, \tag{14}$$

$$D_{SA} = MF_{SA} \cdot D_{rms}. \tag{15}$$

Because the error of SA between the time-series and RVT analyses was minimal for oscillator periods less than 1 s, D_{SA} was considered equal to D_{rms} and MF_{SA} equaled 1. However, for oscillator periods exceeding 1 s, the discrepancy between the time-series analysis and RVT modeling became more significant, and this error was influenced by the oscillator period, magnitude, and source-to-site distance. Furthermore, as can be observed from Figure 2, for $T > 1$ s, the error increases approximately linearly with the period (on a logarithmic scale), and the rate of change in error is influenced by both the M and the R. Therefore, a modification factor MF_{SA} for D_{SA} was proposed

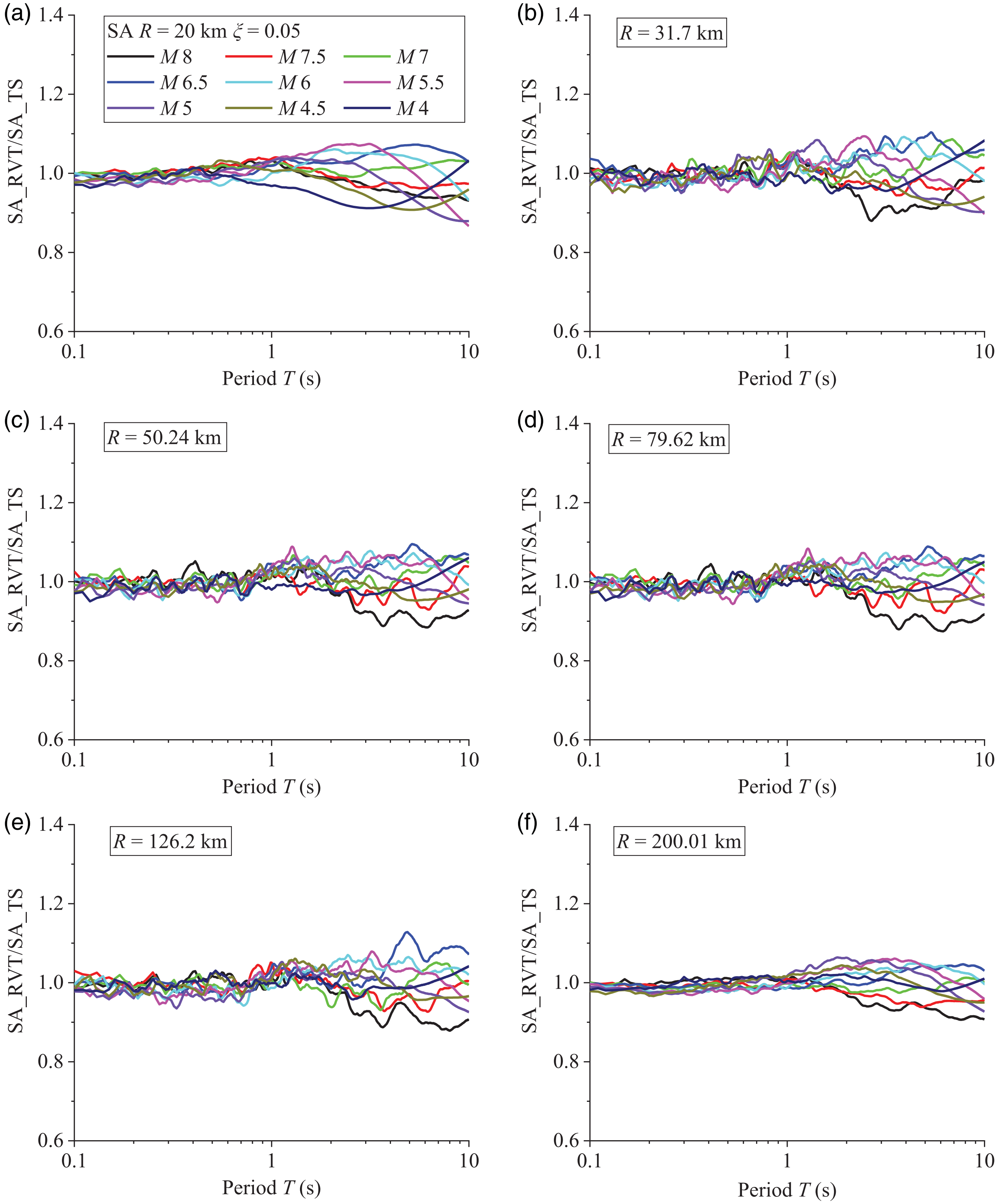

Figure 4. Ratio between SA computed using the proposed approach and time-series analysis considering various magnitudes and distances based on artificial seismic motions.

as a function of the oscillator period, magnitude, and source-to-site distance, expressed in the following form:

$$\mathrm{MF}_{\mathrm{SA}} = 1,(T \le 1)$$
$$\mathrm{MF}_{\mathrm{SA}} = \left(1 + \frac{\log(T)(M-6)(1000-R)}{10^4}\right)^2,(T > 1). \quad (16)$$

For SV, there was a significant discrepancy between the results of the time-series and RVT analyses for oscillator periods exceeding about 0.5 s. This error increased with the period and was affected by the magnitude and source-to-site distance. In addition, as illustrated in Figure 3, for $T > 0.5$ s, the errors exhibit an approximately parabolic growth pattern with respect to the period variation (on a logarithmic scale). Consequently, a modification factor $\mathrm{MF}_{\mathrm{SV}}$ for D_{SV} was also proposed as a function of the oscillator period, magnitude, and source-to-site distance, expressed in the following form:

$$\mathrm{MF}_{\mathrm{SV}} = 1,(T \le 0.5)$$
$$\mathrm{MF}_{\mathrm{SV}} = (k_1 \log T + k_2(\log T)^2 + k_3)^2,(T > 0.5). \quad (17)$$

The parameters k_1, k_2, and k_3 are dependent on the magnitude M and the source-to-site distance R, as listed in Table 2. It is observed that the variation of these parameters with magnitude and source-to-site distance is nonmonotonic. Nevertheless, because the regression analyses covered a wide range of magnitudes and distances with very small intervals relevant to engineering applications, the corresponding values for magnitudes and source-to-site distances not explicitly included in the table can be obtained through interpolation.

COMPARISON OF THE PROPOSED APPROACH WITH THE TIME-SERIES ANALYSIS

Comparison of SA

To validate the effectiveness of the proposed approach for evaluating SA, the ratios of the SA computed by the proposed approach and the time-series analysis are shown in Figure 4. As shown in Figure 4, overall, the results of the proposed approach aligned well with those of the time-series analysis. For periods $T > 1$ s, the discrepancy between the proposed approach and the time-series analysis was consistently less than 10%. By comparing Figures 2 and 4, the error in SA obtained using the proposed approach, when compared to the SA from the time-series analysis, was markedly reduced compared to the cases in which D_{SA} was assumed to be equal to D_{rms}. Furthermore, as the source-to-site distance increased, the error gradually decreased.

To further investigate the accuracy of the proposed approach for calculating SA, 100 real seismic records were selected from strong-motion seismograph networks, K-NET and KiK-net, of Japan. The magnitude M_j (Japan Meteorological Agency magnitude) of these records varies

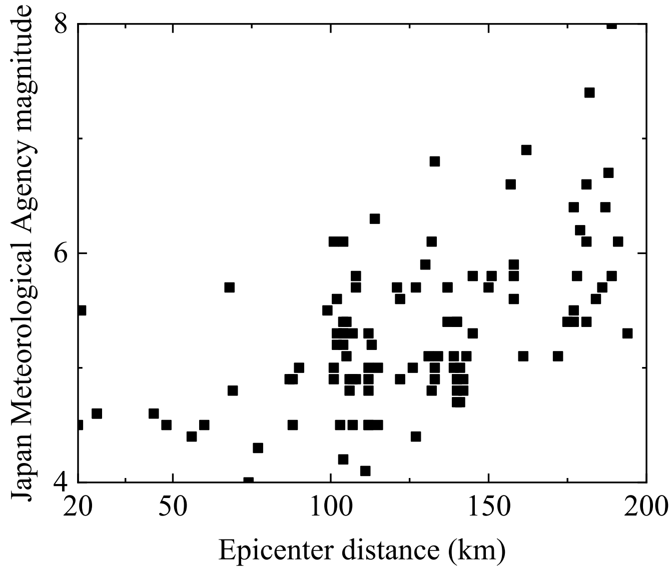

Figure 5. The distribution of magnitude and distance for the selected real earthquake records.

from 4 to 8, and the epicenter distance R_e varies from 20 to 200 km. The magnitude and distance distribution of the selected records is presented in Figure 5. As shown in Figure 5, most of the selected seismic records fall within the range of engineering interest. These seismic records were selected randomly within the aforementioned magnitude and distance ranges to ensure the general applicability of the proposed approach. A baseline adjustment was applied to all records to remove long-period noise. Subsequently, SA values were calculated from the FAS of these seismic records using the proposed approach and compared with those obtained from time-series analysis. Representative comparisons are shown in Figure 6. It can be observed that the SA values calculated by the proposed approach closely match those obtained from time-series analysis. In most cases, the average errors between the proposed approach and time-series analysis are within 10%. In addition, the average ratios of SA calculated by the proposed approach and the time-series analysis, along with the corresponding ± standard deviation, based on 100 real seismic records, are presented in Figure 7. As shown in the figure, the average SA values calculated using the proposed approach are in good agreement with those obtained from time-series analysis, with an average error of approximately 10%. Moreover, the error of the proposed approach shows a slight decrease with increasing period. In contrast, the standard deviation of the SA ratio exhibits a slight increase as the period grows. These phenomena may be attributed to the fact that the proposed approach is developed based on generated time series, which may not fully capture the characteristics of real seismic records. This discrepancy warrants further investigation in future studies.

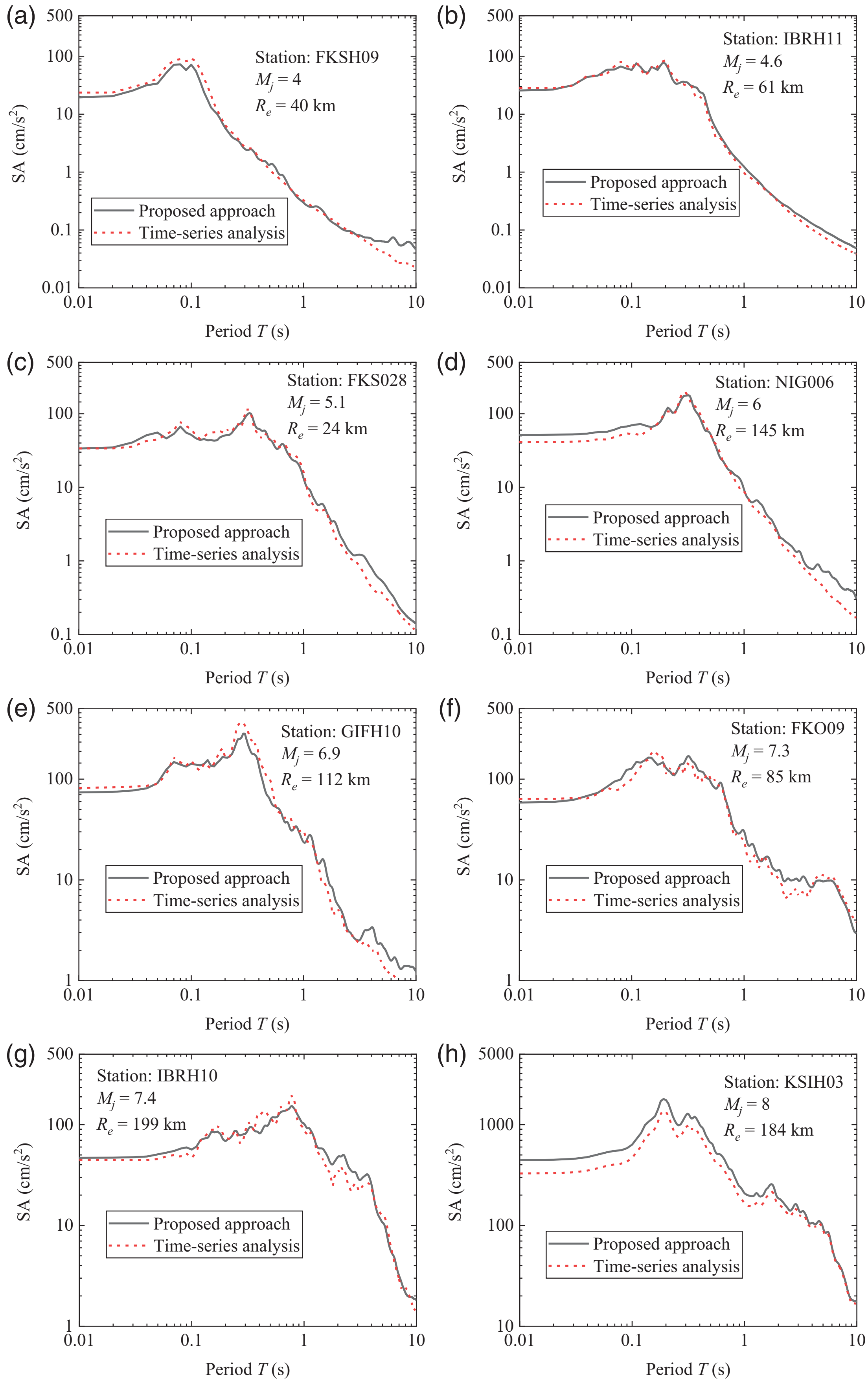

Figure 6. Comparisons of SA results from the proposed approach and time-series analysis using real seismic records.

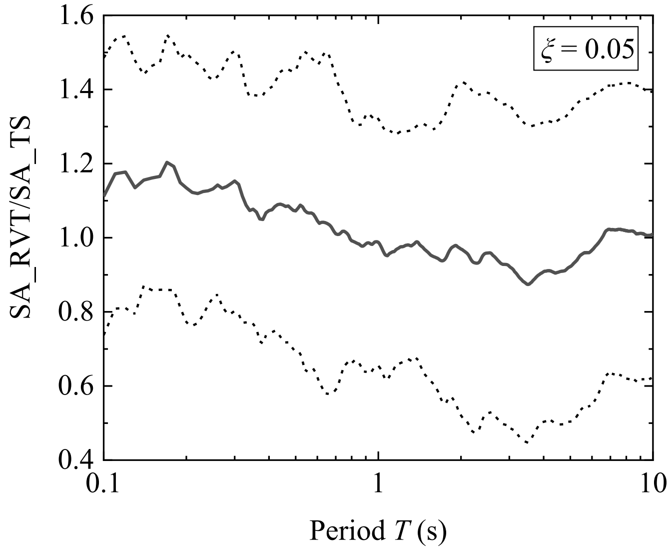

Figure 7. Average ratios of SA calculated using the proposed approach compared to those obtained from time-series analysis, along with the corresponding ± standard deviation, using 100 real seismic records.

Comparison of SV

Figure 8 indicates that the SV calculated using the proposed approach exhibited strong agreement with that calculated from the time-series analysis, with the accuracy improving as the source-to-site distance increased. A comparison of Figures 3 and 8 demonstrated that the SV computed using the proposed approach exhibited closer alignment with that derived from the time-series analysis. In addition, the average relative error between the SV calculated using the proposed approach and that from the time-series analysis was less than 10%. In contrast, when ignoring the differences between D_{rms} and D_{SV}, the average maximum error between the SV obtained through the RVT simulation and that obtained from the time-series analysis was 34.6%.

In addition, SV values were also calculated from the FAS of the 100 real seismic records using the proposed approach and compared with those obtained from time-series analysis. Representative comparisons are presented in Figure 9, showing that the SV values obtained via the proposed approach align closely with those obtained from time-series analysis. In most cases, the average errors are within 10%. In addition, Figure 10 presents the average ratios of SV calculated using the proposed approach compared to those obtained from time-series analysis, along with the corresponding ± standard deviation, using 100 real seismic records. It can be observed that the error of SV in the proposed approach, as well as the standard deviation of the SV ratio, follow a trend similar to that of SA with increasing period. Specifically, the error of SV decreases as the period increases, whereas the standard deviation of the SV ratio exhibits a slight increase with increasing period.

CONCLUSION

This study developed a novel approach for estimating various response spectra from the FAS, including not only SD but also SV and SA, within the framework of RVT. Initially, the equations for estimating SV and SA from the FAS were derived by substituting the oscillator transfer function for SD in the traditional RVT framework with those appropriate for SV and SA, respectively. In addition, two simple modification factors were introduced to adjust the duration of the rms oscillator response, aligning the SV and SA from the RVT modeling with those obtained from the time-series analysis. The proposed approach retains the RVT framework for estimating SD without incorporating new concepts but facilitates the simultaneous estimation of all three types of response spectra. The conclusions are summarized as follows.

1. Ignoring the differences between D_{rms} and D_{SA}, the SA computed using the RVT simulation may exhibit a substantial error from the results obtained via the time-series analysis, with a maximum error of 19.4% at an oscillator period of 10 s. Specifically, for oscillator periods shorter than 1 s, the SA obtained under this assumption closely matched that derived from the time-series analysis. However, when the oscillator period exceeded 1 s, the error increased with the oscillator period and depended on the magnitude and source-to-site distance.
2. Ignoring the differences between D_{rms} and D_{SV}, the SV calculated using the RVT simulation may exhibit a significant error compared with that obtained through the time-series analysis. The error between the two SV values increased with the oscillator period. This error reached 34.6% at an oscillator period of T = 10 s. Furthermore, this error was dependent on the magnitude and source-to-site distance.
3. The SA and SV calculated using the proposed approach demonstrated overall good agreement with the SA and SV from time-series analysis for both artificial seismic motions and real seismic records. Considering various oscillator periods, magnitudes and distances, the average relative error between the results from the proposed approach and those from time-series analysis is found to be limited to approximately 10%.

DATA AND RESOURCES

All data used in this article came from published sources listed in the references.

DECLARATION OF COMPETING INTERESTS

The authors have no conflicts of interest to declare that are relevant to the content of this article to declare.

ACKNOWLEDGMENTS

This study was partially supported by the Japan Society for the Promotion of Science (JSPS) KAKENHI (Grant Number 24K17336),

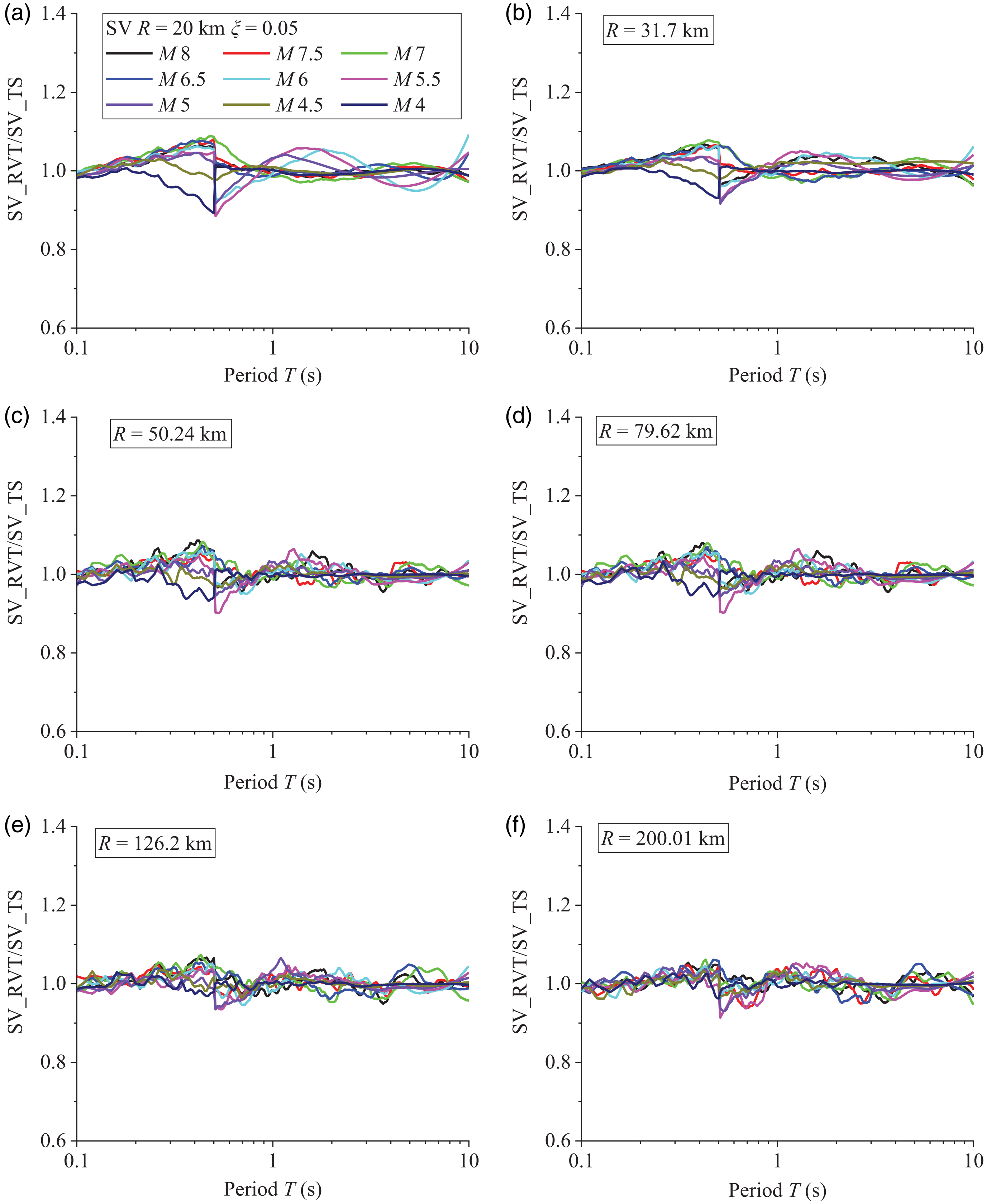

Figure 8. Ratio between SV computed using the proposed approach and time-series analysis considering various magnitudes and distances based on artificial seismic motions.

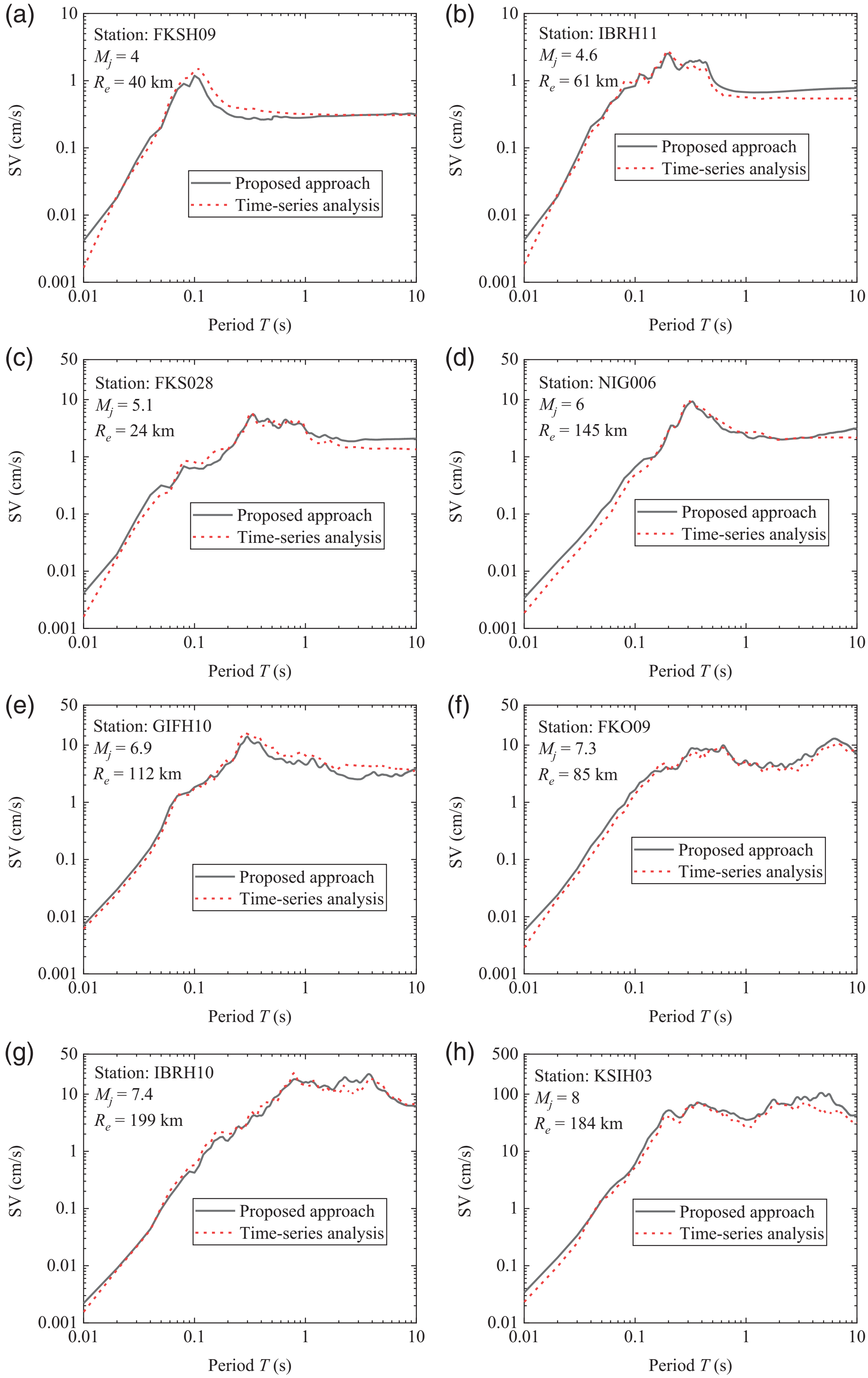

12 **Figure 9.** Comparisons of SV results from the proposed approach and time-series analysis using real seismic records.

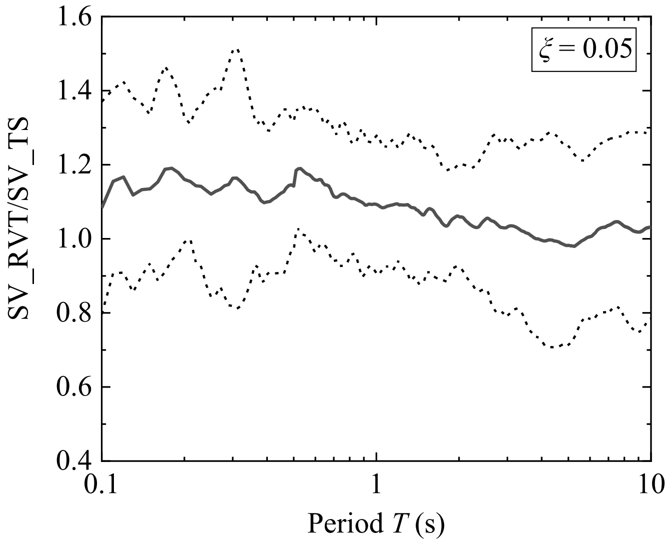

Figure 10. Average ratios of SV calculated using the proposed approach compared to those obtained from time-series analysis, along with the corresponding ± standard deviation, using 100 real seismic records.

the National Natural Science Foundation of China (Grant Number 52278135), and the Qilu Normal University Research Start-Up Fund. The authors sincerely appreciate this support. In addition, the authors would like to express their gratitude to the reviewers and the associate
3 editor for their valuable comments and suggestions, which have helped improve this article. All data generated or analyzed during this study are included in this published article. Code availability is available upon request. All authors contributed to the study conception and design. Data curation, writing-original draft preparation, visualization, conceptualization, and methodology were performed by Rui Zhang, Haizhong Zhang, and Yan-Gang Zhao. The first draft of the article was written by Rui Zhang and all authors commented on previous versions of the article. All authors read and approved the final article.

REFERENCES

ASCE/SEI7-10 (2011). *Minimum Design Loads for Buildings and Other Structures*, Structural Engineering Institute (SEI), American Society of Civil Engineers (ASCE), Reston, Virginia.

Atkinson, G. M., and D. M. Boore (2014). The attenuation of Fourier amplitudes for rock sites in eastern North America, *Bull. Seismol. Soc. Am.* **104,** 513–528.

Atkinson, G. M., and W. Silva (2000). Stochastic modeling of California ground motions, *Bull. Seismol. Soc. Am.* **90,** 255–274.

Boore, D. M. (2003). Simulation of ground motion using the stochastic method, *Pure Appl. Geophys.* **60,** 635–676.

Boore, D. M. (2005). SMSIM—Fortran programs for simulating ground motions from earthquakes: version 2.3-A revision of OFR 96-80-A, *U.S. Geol. Surv. Open-File Rept. 00-509*.

Boore, D. M., and G. M. Atkinson (1987) Stochastic prediction of ground motion and spectral response parameters at hard-rock sites in eastern North America, *Bull. Seismol. Soc. Am.* **72,** no. 2, 440–467.

Boore, D. M., and W. B. Joyner (1984). A note on the use of random vibration theory to predict peak amplitudes of transient signals, *Bull. Seismol. Soc. Am.* **74,** 2035–2039.

Boore, D. M., and E. M. Thompson (2012). Empirical improvements for estimating earthquake response spectra with random-vibration theory, *Bull. Seismol. Soc. Am.* **102,** 761–772.

Boore, D. M., and E. M. Thompson (2015). Revisions to some parameters used in stochastic-method simulations of ground motion, *Bull. Seismol. Soc. Am.* **105,** no. 2A, 1029–1041.

Boore, D. M. (1983). Stochastic simulation of high-frequency ground motions based on seismological models of the radiated spectra, *Bull. Seismol. Soc. Am.* **73,** no. 6A, 1865–1894.

Bora, S. S., F. Scherbaum, and N. Kuehn (2014). Fourier spectral- and duration models for the generation of response spectra adjustable to different source-, propagation-, and site conditions, *Bull. Earthq. Eng.* **12**, no. 1, 467–493

Bora, S. S., F. Scherbaum, and N. Kuehn (2016). On the relationship between Fourier and response spectra: implications for the adjustment of empirical ground-motion prediction equations (GMPEs), *Bull. Seismol. Soc. Am.* **106,** no. 3, 1235–1253.

Campbell, K. W. (2003). Prediction of strong ground motion using the hybrid empirical method and its use in the development of ground-motion (attenuation) relations in Eastern North America, *Bull. Seismol. Soc. Am.* **93,** no. 3, 1012–1033.

Cartwright, D. E., and M. S. Longuet-Higgins (1956). The statistical distribution of the maxima of a random function, *Proc. Math. Phys. Sci.* **237,** 212–232.

Conde-Conde, J., and A. Benavent-Climent (2019). Construction of elastic spectra for high damping, *Eng. Struct.* **191,** 343–357.

Davenport, A. G. (1964). Note on the distribution of the largest value of a random function with applications to rust loading, *Proc. Inst. Civ. Eng.* **28,** no. 2, 187–196.

Desai, R. S., and S. N. Tande (2017). Estimation of spectral velocity at long periods for application in velocity dependant seismic energy management devices, *J. Struct. Eng.* **44,** no. 1, 14–22.

Eurocode 8 (2004). Design of structures for earthquake resistance, part 1: General rules, seismic actions and rules for buildings, *EN 2004–1–1*, European Committee for Standardization (CEN), Brussels, Belgium.

Federal Emergency Dissipation Agency (FEMA-450) (2003). NEHRP recommended provisions for seismic regulations for new buildings and other structures. Part 1: Provisions and Part 2: Commentary, *FEMA P-2082-1*, Washington, D.C.

Fujiwara, H., S. Kawai, and S. Aoi (2006). National seismic hazard maps for Japan, *Bull. Earthq. Res. Inst.* **81,** 221–232.

GB 18306-2015 (2015). *Seismic Ground Motion Parameters Zonation Map of China*, China Building Industry Press, Beijing, China (in Chinese).

GB 50011-2010 (2016). *Code for Seismic Design of Buildings*, China Building Industry Press, Beijing, China (in Chinese).

Hanks, T. C., and R. K. McGuire (1981) The character of high-frequency strong ground motion, *Bull. Seismol. Soc. Am.* **71,** no. 6, 2071–2095.

Herrmann, R. B. (1985) An extension of random vibration theory estimates of strong ground motion to large distances, *Bull. Seismol. Soc. Am.* **75,** no. 5, 1447–1453.

Kottke, A. R., N. A. Abrahamson, and D. M. Boore (2021). Selection of random vibration theory procedures for the NGA-East project and ground-motion modeling, *Earthq. Spectra* **37,** 1420–1439.

Lavrentiadis, G., and N. A. Abrahamson (2023). A non-ergodic spectral acceleration ground motion model for California developed with random vibration theory, *Bull Earthq Eng.* **21,** 5265–5291.

Liu, L., and S. Pezeshk (1999). An improvement on the estimation of pseudo response spectral velocity using RVT method, *Bull. Seismol. Soc. Am.* **89,** 1384–1389.

Liu, Z., Y. G. Zhao, and H. Z. Zhang (2025). Estimation of velocity response spectrum using acceleration response spectrum, *Mech. Syst. Signal. Process.* **223,** 111,909.

4 PEER Report (2015). NGA-East: median ground-motion models for the central and Eastern North America region, *PEER Report 2015-04*, Pacific Earthquake Engineering Research Center, University of California, Berkeley, California, available at https://peer.berkeley.edu/sites/default/files/webpeer-2015-04_nga-east-_median_ground-motion_models_for_the_central_and_eastern_north_america_region.pdf.

Rathje, E. M., and M. C. Ozbey (2006). Site-specific validation of random vibration theory-based seismic site response analysis, *J. Geotech. Geoenviron. Eng.* **132,** no. 7, 911–922.

Toro, G. R., and R. K. McGuire (1987). An investigation into earthquake ground motion characteristics in eastern North America, *Bull. Seismol. Soc. Am.* **77,** no. 2, 468–489.

Vanmarcke, E. H. (1975). Distribution of first-passage time for normal stationary random processes, *J. Appl. Mech.* **42,** 215–220.

Wang, X., and E. M. Rathje (2016). Influence of peak factors on site amplification from random vibration theory based site-response analysis, *Bull. Seismol. Soc. Am.* **106,** no. 4, 1–14.

Yu, R. F., and X. Y. Zhou (2008). Response spectrum analysis for non-classically damped linear system with multiple-support excitations, *Bull. Earthq. Eng.* **6,** 261–284.

Zhang, H. Z., and Y. G. Zhao (2020). Damping modification factor based on random vibration theory using a source-based ground-motion model, *Soil. Dynam. Earthq. Eng.* **136,** 106,225.

Zhang, H. Z., and Y. G. Zhao (2021a). Damping modification factor of acceleration response spectrum considering seismological effects, *J. Earthq. Eng.* **26,** no. 20, 1–24.

Zhang, H. Z., and Y. G. Zhao (2021b). Effects of earthquake magnitude, distance, and site conditions on spectral and pseudospectral velocity relationship, *Bull. Seismol. Soc. Am.* **111,** 3160–3174.

Zhang, H. Z., and Y. G. Zhao (2021c). Analytical model for response spectral ratio considering the effect of earthquake scenarios, *Bull. Earthq. Eng.* **19,** 5285–5305.

Zhang, H. Z., and Y. G. Zhao (2022). Effects of magnitude and distance on spectral and pseudospectral acceleration proximities for high damping ratio, *Bull. Earthq. Eng.* **20,** 3715–3737.

Zhang, R., Y. G. Zhao, and H. Z. Zhang (2023). An efficient method for probability prediction of peak ground acceleration using Fourier amplitude spectral model, *J. Earthq. Eng.* **28,** no. 6, 1495–1511.

Zhao, Y. G., R. Zhang, and H. Z. Zhang (2023). Probabilistic prediction of ground-motion intensity for regions lacking strong ground-motion records, *Soil. Dynam. Earthq. Eng.* **165,** 107,706.

Zhou, X. Y., R. F. Yu, and D. I. Dong (2004). Complex mode superposition algorithm for seismic responses of non-classically damped linear MDOF system, *J. Earthq. Eng.* **8,** no. 4, 597–641.

Manuscript received 4 October 2024